Deploying, Scheduling and Sequencing Heterogeneous Vessels in a Liner Container Shipping Route

Abstract

Previous studies on liner container shipping operations usually assume identical container ships that are deployed in the same shipping route. However, in real operations, this assumption does not always hold considering the distinct capacities, ages, fuel efficiencies, cost structures, etc. of these ships. These distinctions of the ships significantly influence the number of containers transported, the freight revenue, and the operating cost. In this regard, this paper considers the joint ship deployment, sequencing, and scheduling problem for a fleet of heterogeneous vessels in a shipping route. A mixed integer programming model is developed to select the optimal ships from a set of candidate ships together with their sequences, schedules, and sailing speeds in the shipping route to minimize the total cost. A tailored solution algorithm is subsequently developed to calculate the global optimal solution very efficiently. A series of numerical experiments demonstrate that this algorithm significantly outperforms the classical branch-and-cut algorithm in solving the model. In addition, by applying our model in a real-case shipping route, we find that the model is able to reduce the total cost by 3% compared with the model considering homogenous vessels. Finally, several managerial insights are obtained to guide the operations of a liner shipping route.

Keywords: liner container shipping, fleet deployment, ship scheduling, heterogeneous vessels, global optimization

1. Introduction

Container shipping is the backbone of the global logistics system that connects the trades between different continents. It is reported by UNCTAD (2019) that the volume of containerized cargo has seen a 5.8% annual growth in the past two decades and the total container trade volume reached 152 million TEUs (20-foot equivalent units) in 2018. Liner shipping provides container shipping service by a fleet of container ships that follow fixed routes and schedules. In a shipping route, the container ships call a sequence of ports with a fixed frequency, usually once a week (Agarwal and Ergun, 2008), to transport the containers. To achieve an efficient shipping service, the liner operators must deploy the most appropriate ships in the route and determine their visit schedules for all ports of call. For ease of modeling and solving the fleet deployment and scheduling (FDS) problem, current studies usually assume identical container ships in the same route (Wang and Meng, 2017). However, in real operations, this assumption does not hold because these ships cannot be identical considering the distinct capacities, cost structures, ages, etc. in different ships. Here we identify the following two important factors that distinguish these ships.

First, the capacities may vary for ships in the same route. This may be because these ships are built at different times or come from different shipping companies in an alliance. Take the Asia-Europe service AEU1 operated by COSCO as an example. This service has ten ships deployed with their capacities ranging between 13300 TEUs and 21413 TEUs (COSCO, 2020), a variation of 37.9%. In general, larger ships can transport more containers but incur higher operating costs. On the contrary, deploying smaller ships leads to lower operating costs, but the shipping company has to purchase more third-party slots from other shipping companies for the unsatisfied shipping demand and thus has higher slot purchase costs. Therefore, given a set of container ships that differ in capacities and operating costs, a wise selection of ships to deploy in the shipping route has a significant effect on the operating cost and the freight revenue of the shipping route.

Second, these ships also differ in bunker fuel consumption rates. Fig. 1 depicts the bunker consumption functions of two ships belonging to the same shipping route with respect to sailing speeds that are calibrated on actual ship log data. We can see that these two functions

have quite different trends in terms of the variations in sailing speed. The difference in the bunker consumption rates can be as large as 48.1% (when the sailing speed is 10 knots). There exist several reasons accounting for different bunker consumptions among the ships in the same route. First, as mentioned above, these ships may have different capacities. In general, the larger the ship size, the higher the bunker consumption. Second, ships may be built with different manufacturing techniques and thus have different mechanical performance and bunker consumption efficiency. Third, even the fuel consumption rate of the same ship may vary in operation. This is, the ship may wear out as time goes by, which increases the fuel consumption rate. At the same time, the scheduled maintenance of the ship, on the contrary, could improve fuel efficiency and reduce fuel consumption. As the bunker consumption cost takes up the largest part of the total ship operating cost (Ronen, 2011), the variation of sailing speed can significantly change the operating cost of these ships and thus influence the ship selections. Therefore, it is vital for the liner operators to consider the optimal ship sailing speed and the ship schedules when deploying heterogeneous ships in order to reduce the operating cost of the shipping route.

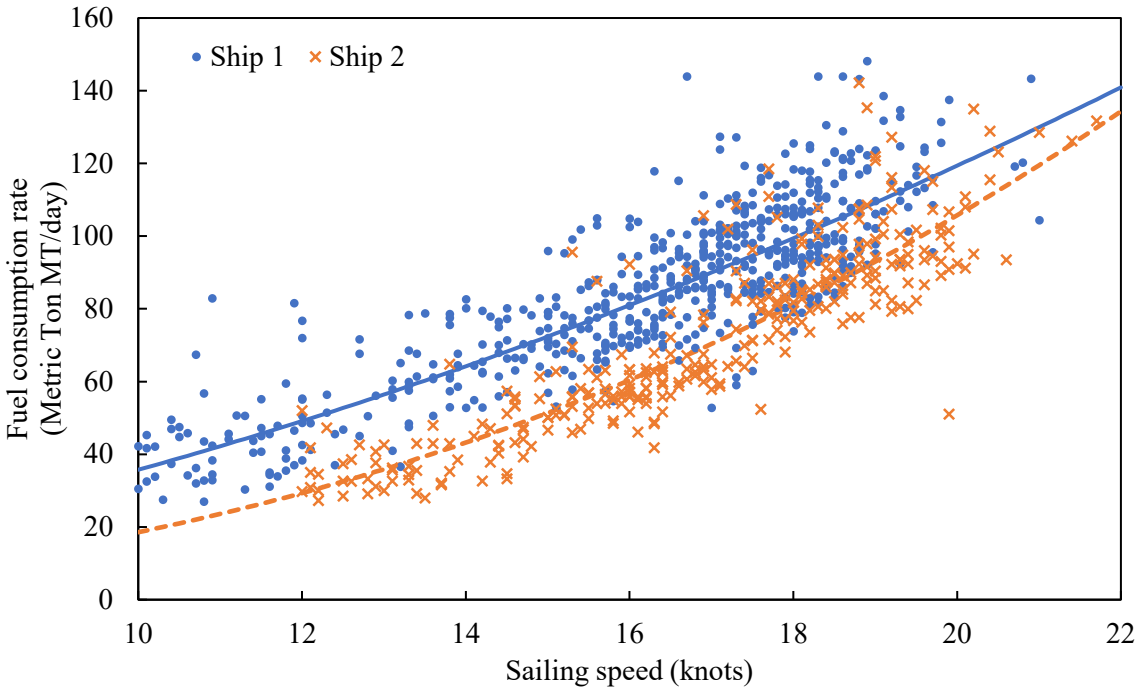

Fig. 1 Fuel consumption function of two ships in the same shipping route

In addition, extant studies usually consider fixed container shipping demand across the planning horizon when solving the FDS problem. However, in reality, due to factors such as the global economy, the production plan of the manufacturers, and seasonality factors (e.g., Christmas, Chinese New Year), remarkable variations of the shipping demand volume exist across the planning horizon. Fig. 2 below can be viewed as evidence that indicates considerable fluctuations of container shipping demand of four origin-destination (OD) pairs across a whole year. Given the weekly-dependent shipping demand, there is a need to optimize the sequence of the ships with different capacities in the shipping route. This is because large ships are preferable when the shipping demand is high in some weeks while small ships are more appropriate for low shipping demand in other weeks. Therefore, arranging these ships with different capacities to match these weekly-dependent demands can increase the utilization of the ship capacity and thus improve the profitability of a shipping company.

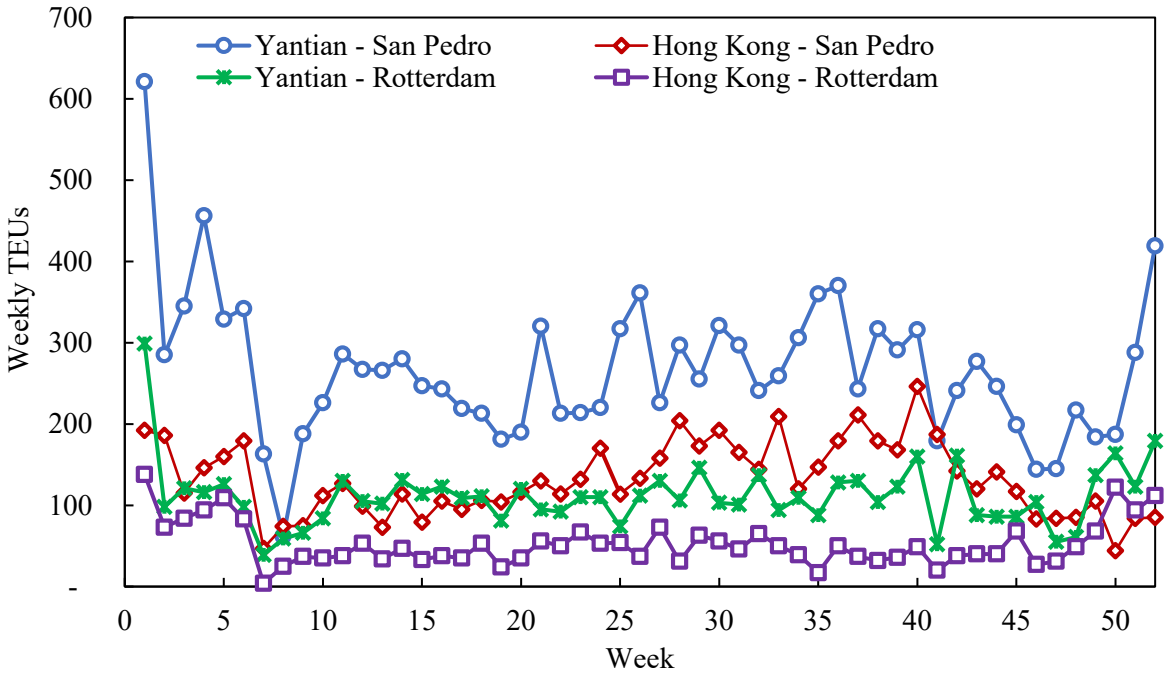

Fig. 2. Container shipping demand variations for 4 OD pairs (Wang, 2015)

Based on the above considerations, this paper investigates how to deploy, schedule, and sequence a fleet of heterogeneous ships under weekly-dependent shipping demand to minimize the total cost which is the sum of the ship operating cost, the bunker consumption cost, and the penalty cost for the unsatisfied shipping demand. This problem can be referred to as the

deploying, scheduling, and sequencing (DSS) problem for the heterogeneous liner shipping vessels. The DSS problem simultaneously deals with the following three issues:

i) (*Deployment*) Given a set of candidate ships that differ in capacity, operating cost, and bunker fuel consumption, the DSS problem needs to select and deploy optimal ships in the shipping route through balancing the containers transported by the ships and the corresponding operating costs.

ii) (*Scheduling*) The DSS problem needs to determine the optimal sailing speeds in all shipping legs and the visit schedules for the ports of call in the route. For a stable service with fixed service frequency, the sailing speeds of all ships deployed in the route should be identical in each shipping leg.

iii) (*Sequencing*) Considering the variations of container shipping demand in the planning horizon, the DSS problem needs to determine the sequence of these heterogeneous ships deployed in the shipping route so that the capacities of the ships can match the weekly-dependent container shipping demands.

The above three issues are interrelated. That is, scheduling ships relates to the optimization of sailing speed and the bunker consumption cost, which further affects the selection and deployment of ships in the shipping route from the candidate set. In addition, the deployment of heterogeneous ships also induces the need to determine the sequence of these ships to accommodate the weekly-dependent shipping demand. To tackle the DSS problem, this paper first formulates this problem as a mixed integer linear programming (MILP) model. Due to the large size of this model, it cannot be solved by the classical branch-and-cut (B&C) algorithm implemented in commercial solvers in a short time. Hence, a tailored solution algorithm is developed in this study that is able to solve the model efficiently in a short time. A series of numerical experiments are conducted to compare the efficiency of the algorithm with that of the B&C. Results demonstrate that this algorithm can be dramatically faster than the B&C to solve real-sized problems.

2. Literature Review

The topic of this paper is related to two research areas in liner shipping that have been extensively discussed in the literature, that is, fleet deployment and vessel scheduling. We first review studies on fleet deployment and then turn to vessel scheduling. Please note that considering the length of this paper, we cannot provide an exhaustive literature review but select some typical studies in these two areas. The detailed review can be seen in Wang and Meng (2017) and Dulebenets et al. (2019).

The fleet deployment problem considers how to assign ships of different types to shipping routes in order to minimize the total ship operating cost. To the authors' knowledge, the earliest studies on fleet deployment date back to Benford (1981) and Perakis (1985). Benford (1981) develops a simple procedure to select the best mix of ships and the speeds for a shipping route with only two ports to maximize the profit of the shipowner. Perakis (1985) further formulates the problem in Benford (1981) as a programming model and solves it by the Lagrange multiplier method. Inspired by these two pioneering works, many subsequent studies discuss fleet deployment as a standalone problem (e.g., Powell and Perakis, 1997; Meng and Wang, 2010; Ng, 2014; Ng, 2015) or together with other problems such as container routing (e.g., Fagerholt et al, 2009; Meng et al., 2012; Wang and Meng, 2012a; Monemi and Gelareh, 2017; Zhen et al, 2019), sailing speed optimization (e.g., Gelareh and Meng, 2010; Pasha et al., 2020), network design (e.g., Agarwal and Ergun, 2008; Alvares, 2009; Song and Dong, 2013; Brouer et al, 2014; Xia et al., 2015; Wang et al., 2019), and green shipping (e.g., Zhu et al., 2018; Cheaitou and Cariou, 2019; Zhen et al., 2020). For example, Alvares (2009) considers the joint routing and deployment of container vessels that service several ports to minimize the operating costs of a liner shipping company over a planning horizon. A tabu search algorithm embedded with a column generation technique is developed to solve this problem. A mixed integer programming model is formulated in Gelareh and Meng (2010) to determine the optimal ship type deployed and the sailing speed in each route of the shipping network. Meng and Wang (2010) solve the short-term liner ship fleet deployment problem under the uncertain container shipping demand. Chance constraints are adopted to guarantee that the deployed ships should satisfy the shipping demand with a predetermined probability. Considering that

the shipping demand may vary significantly during the planning horizon, Meng and Wang (2012) investigate the ship fleet deployment with the weekly-dependent container shipping demand. A time-space network is constructed to help model the routing of container shipping demand in each week of the planning horizon. This paper also takes into account the weekly-dependent demand to reflect the shipping demand fluctuations in the planning horizon. Song and Dong (2013) design a long-haul liner service route with the joint consideration of fleet deployment and empty container repositioning. Ng (2014) considers the liner shipping vessel deployment with the distribution-free uncertain shipping demand. In that paper, only the mean, standard deviation, and upper bound are needed for the uncertain demand, which can be easy to obtain in practice. Pasha et al. (2020) consider the holistic tactical-level planning in liner shipping that jointly optimizes service frequency, fleet deployment, ship sailing speed, and schedule. As the environmental impacts of maritime shipping are attracting more and more attention in both academia and industry, some studies discuss the fleet deployment problem in the context of green shipping. For example, Zhu et al. (2018) investigate the impact of the emission trading system on the container ship fleet deployment. By examining real data from the industry, they find that the trading system can motivate shipping companies to deploy more "energy-carbon-efficient" ships and lay up energy-inefficient ships. Zhen et al. (2020) optimize the green technology adoption strategy for a container ship fleet in response to the establishment of emission control areas (ECAs). Two potential technologies are considered, i.e., the gas scrubbers and the shore power.

Another research area that this paper is related to is the liner shipping vessel scheduling problem that aims to determine the sailing speed in each shipping leg and the arrival and/or departure time at each port of call. Considerable studies have been conducted to discuss this problem in recent decades (e.g., Fagerholt, 2001; Ronen 2011; Wang and Meng, 2012b; Song et al., 2015; Fagerholt et al., 2015; Wang et al., 2015; Aydin et al., 2017; Dulebenets and Ozguven, 2017; Tan et al., 2018; Wang et al., 2018; Giovannini and Psaraftis, 2019; Gürel and Shadmand, 2019; Wang et al., 2019; Abioye et al. 2020; Wang and Meng, 2020). Fagerholt (2001) designs the ship schedules that allow ships to violate the port time windows at the expense of violation inconvenience costs. A number of feasible routes and schedules are first

enumerated for a number of ships. A set partitioning problem is then constructed to select the optimal routes and schedules for these ships to minimize the total route cost. Ronen (2011) shows that the bunker consumption cost could constitute more than 75% of the total operating costs. Reducing the sailing speed leads to a lower operating cost but increases the round-trip time of the route and thus the fleet size in the route to maintain the fixed service frequency. A nonlinear programming model is constructed to analyze this trade-off and a simple procedure is provided to solve the model to obtain the optimal sailing speed and fleet size. Song et al. (2015) jointly plan the fleet size, ship sailing speed, and the service schedule in order to optimize three objectives, i.e., expected cost, service reliability, and ship emissions considering the port time uncertainty. This problem is solved by a simulation-based non-dominated sorting genetic algorithm. Fagerholt et al. (2015) examine the effects of the ECAs on the ship sailing speed, schedule, and ship route. Results show that with the establishment of the ECAs, a ship will choose to sail a longer distance away from the ECAs and the sailing speed within the ECAs is generally lower than that outside. Aydin et al. (2017) optimize the ship sailing speed under uncertain port times and time windows to minimize the total fuel consumption while maintaining schedule reliability. Dulebenets and Ozguven (2017) design the vessel schedule in a liner shipping route with perishable assets. A mixed integer nonlinear programming model is constructed and then linearized by a piece-wise linear secant approximation method. The linearized model is solved by CPLEX. Tan et al. (2018) design the schedule of an inland river liner shipping service by considering the stochastic dam transit time. A Pareto optimization model is constructed that optimizes the total round-trip time and fuel consumption simultaneously. Wang et al. (2019) consider a single intercontinental liner shipping service design problem that simultaneously determines the shipping route, the ship sailing speed and schedule, and the container routing for each OD pair to maximize the total profit. A tailored branch-and-cut-and-Benders algorithm is developed to solve this problem. Different from previous papers that assume weekly service frequency, Giovannini and Psaraftis (2019) optimize ship sailing speed and service frequency for a shipping route to maximize the average daily profit. Results show that allowing variable service frequency leads to lower operating costs and CO_2 emissions. Gürel and Shadmand (2019) solve the scheduling problem for the

heterogenous ship types considering uncertainties in port time. Abioye et al. (2020) consider the liner shipping schedule recovery problem through four strategies including adjusting sailing speed, adjusting vessel handling rate, skipping ports with/without container diversion. A nonlinear programming model is formulated for this problem and is solved by the nonlinear optimization solver BARON.

Despite considerable articles addressing the liner shipping fleet deployment and scheduling, most of them assume that the container ships deployed in a shipping route are identical. As far as the authors are concerned, there are only two studies considering the heterogeneous fleet, i.e., Wang (2015) and Dulebenets (2018). Wang (2015) investigates how to arrange ships in a route that differ in capacities considering the fluctuations of weekly shipping demand. Three heuristic rules are given to determine the permutations of these ships that are quite close to the optimal permutation. However, that study only considers a shipping route with only two ports (one export port and one import port) which restricts its application in real operations. In addition, the ship deployment and sailing speed optimization are not considered in that study. Dulebenets (2018) considers the vessel scheduling problem with a heterogeneous fleet. In that paper, the shipping route allows container ships with different bunker consumptions, port handling costs, and operating costs. However, that paper assumes that the shipping demand does not change in the planning horizon and it cannot determine the exact sequence of these heterogeneous ships to accommodate the time-varying shipping demand in real operations. To fill this gap, this paper considers the DSS problem in a liner shipping route that simultaneously optimizes the deployment, schedule, and sequence of a fleet of heterogeneous ships under weekly-dependent shipping demand. Therefore, the problem in this paper is more general and applicable than those in Wang (2015) and Dulebenets (2018) as it incorporates more practical considerations.

The contributions of this paper can thus be stated as follows. First, this paper considers the joint deployment, scheduling, and sequencing problem for a fleet of heterogeneous ships in a shipping route under weekly-dependent shipping demand, which has never been discussed in the literature. Second, to tackle this problem, a mixed integer linear programming model is developed to select the optimal ships from the candidate set of ships and determine the optimal

sailing speed, schedule, and sequence of these ships in order to minimize the total cost of the shipping route. Third, considering the large size of this programming model, a tailored solution algorithm is developed to obtain the global optimal solution in a short time. Numerical experiments show that this algorithm is much faster than the classical B&C algorithm in solving the model.

The remainder of this paper is organized as follows. Second 3 elaborates the problem considered in this paper and constructs a mixed integer linear programming model for the problem. Section 4 develops a tailored solution algorithm to obtain the global optimal solution of the model. Numerical experiments are conducted in Section 5 to test the efficiency of the solution algorithm and the applicability of the model. Finally, Section 6 gives the conclusions of this paper and the recommendations for future research.

3. Model Formulation

Consider a liner container shipping company that operates a shipping route and has a set of candidate container ships that can be deployed in this route. The shipping company needs to determine which ships are selected to deploy in the route together with their schedules and sequences in the planning horizon. In this section, a mixed integer nonlinear programming model is first formulated for this problem. This model is then transformed into a mixed integer linear programming model which can be solved by the existing commercial solvers. The notations used in this paper are listed in Table 1.

Table 1. Notations

Sets	
D	Set of all OD pairs
I	Set of all ports and legs, $I = \{1,2,...,N\}$
I_{ij}	Set of all ports and legs in the route from port i to port j.
S	Set of all available vessels
Parameters	
Cap_s	Capacity of ship $s \in S$
c^{bunk}	Bunker fuel price
c_s^{oper}	Weekly operating cost of ship $s \in S$
c_{od}	Penalty cost per TEU for unsatisfied shipping demand

l_i	Length of shipping leg $i \in I$ (nautical mile)
T	length of the planning horizon in weeks
t_i^p	Port stay time in port $i \in I$
$v_i^{\max}, v_i^{\min}$	Maximum and minimum sailing speed in leg $i \in I$
α_i^s, β_i^s	Parameters of bunker consumption function of ship $s \in S$ in leg $i \in I$
ξ_{od}^k	Container shipping demand in week *k* and $(o,d) \in D$
Variables	
m	Number of ships deployed in the service
t_i	Vessel traveling time in leg $i \in I$
v_i	Vessel sailing speed in leg $i \in I$
x_s	Binary indicating whether ship *s* is deployed
x_k^s	Binary indicating whether ship $s \in S$ is deployed in week $k = 1,2,...,T,...,T+m$
y_{od}^k	Number of containers loaded in week *k* for demand $(o,d) \in D$
z_{od}^k	Number of containers transported by third-party services in week k for demand $(o,d) \in D$
θ_τ^{ji}	Binary indicating whether the ship visit port *i* from port *j* in τ weeks
Auxiliary Variables	
B_i^s, C_i^s	Auxilliary nonnegative variables to linearize objective function (17)
$g_{od}^{ki\tau}, q_s^{ki\tau}$	Auxilliary nonnegative variables to linearize constraint set (7)
n_i	Auxilliary integer variable to linearize constraint set (10)

3.1 Ship Schedule and Weekly Service Frequency

In this paper, we assume that the port rotations of the route are pre-determined. Denote by *I* the set of all ports of call in the route. The route is a cycle of all ports of call and can thus be expressed as $1 \to 2 \to ... \to i \to ... \to |I| \to 1$, where 1 represents the first port of call, and $|I|$ is the number of ports of call in the route and also represents the last port of call. A shipping leg is defined as the voyage between two adjacent ports of call and, for ease of presentation, is also numbered by its starting port of call $i \in I$. To keep a fixed service frequency, the sailing time in each shipping leg should be identical among all deployed ships. Denote by the decision variable t_i (hour) the sailing time in leg $i \in I$ and the constant l_i (nautical mile, nm) the leg distance. The sailing speed in the shipping leg *i* can be easily calculated as $v_i := l_i / t_i, \forall i \in I$ (knot). The sailing time should fall in a feasible range in practice:

$$t_i \in [l_i / v_i^{\max}, l_i / v_i^{\min}], \forall i \in I \quad (1)$$

where $v_i^{\max}$ (knots) and $v_i^{\min}$ (knots) are the largest and smallest economic sailing speed in the shipping leg *i* respectively. We assume that the ships deployed in the route should maintain weekly service frequency for all ports of call in the route. Hence, the following constraint set should be satisfied:

$$\sum_{i \in I} (t_i^p + t_i) = 168m \quad (2)$$

where the term t_i^p (hour) represents the port-stay time at port of call $i \in I$ including vessel waiting time, vessel pilotage in and out time, and cargo handling time, and is assumed to be constant in this paper; the decision variable $m \in Z_+$ refers to the number of ships deployed in the shipping route; 168 is the number of hours in a week.

3.2 Vessel Deployment and Sequencing Constraints

Denote by S the set of all candidate ships and *T* the total number of weeks in the planning horizon. For each ship *s* in the set *S*, we let the binary decision variable x_s indicate whether the ship *s* will be deployed in the route and the binary decision variable x_s^k indicate whether the ship *s* will start the voyage from the first port of call 1 in week $k \in \{1,...,T\}$. We have the following constraints for the two variables:

$$x_s = \sum_{k=1}^{m} x_s^k, \forall s \in S \quad (3)$$

$$\sum_{s \in S} x_s^k = 1, \forall k \in \{1,...,T\}. \quad (4)$$

Constraint set (3) indicates that if ship *s* is deployed in the route, it must start its voyage between week 1 and week *m*. Constraint set (4) indicates that there should be only one ship that starts its voyage in each week *k.* As a ship finishes the whole voyage in *m* weeks, it should start a new voyage every *m* weeks. Therefore, the following constraint set is valid.

$$x_s^k = x_s^{(k-1) \bmod m+1}, \forall k = 1,...,T, s \in S \tag{5}$$

where the operator "mod" calculates the remainder when k is divided by m.

3.3 Weekly-dependent Shipping Demand and Ship Capacity Constraints

In this paper, we assume that the shipping demand is classified by the OD pair and each type of shipping demand varies in different weeks. Denote by D the set of all OD pairs and ξ_{od}^k (TEU) the number of containers of type $(o,d) \in D$ to transport in week k which is assumed to be precisely predicted and thus fixed. We also let the nonnegative decision variable y_{od}^k (TEU) represent the number of containers to load onboard in week k for demand $(o,d) \in D$. Due to the ship capacities, the shipping route may not be able to transport all containers. The unsatisfied shipping demand will be transported by other shipping routes of the shipping company itself or other companies, which is represented by a nonnegative decision variable z_{od}^k (TEU). We thus have the following constraint set.

$$y_{od}^k + z_{od}^k \geq \xi_{od}^k, \forall (o,d) \in D, k \in \{1,...,T\}. \tag{6}$$

As the shipping route maintains weekly service frequency, there should be one and only one ship visiting port of call i and then sailing through the shipping leg i in each week k, which can be represented by the tuple (i,k). For each tuple (i,k), we have the following shipping capacity constraints

$$\sum_{\substack{(o,d) \in D \\ i \in I_{od}}} \sum_{\tau=0}^{\min(m,k-1)} y_{od}^{k-\tau} \theta_\tau^{oi} \leq \sum_{s \in S} \sum_{\tau=0}^{\min(m,k-1)} x_s^{k-\tau} \theta_\tau^{1i} Cap_s, \forall i \in I, k \in \{1,...,T+m\} \tag{7}$$

where the function $\min(\cdot,\cdot)$ returns the minimum value of two numbers, and the variable θ_τ^{ji} is defined to be a binary variable that equals 1 if and only if a ship visits the port j in week k and then visits port i in week $k+\tau$. For example, if a ship visits port 1 in week 1 and visits port 2 in week 3, then the variable $\theta_2^{12} = 1$. Also note that as there are m ships deployed in the route, it takes m weeks for a ship to finish the whole round-trip voyage of the route and thus

$\tau \in \{0,1,...,m\}$. The left-hand side of (7) represents the total number of containers that are transported by the ship indicated by the tuple (i,k), i.e., visiting port of call *i* and sailing through the shipping leg *i* in each week *k*. For example, for the ship visiting port 2 and the leg 2 in week 3, if $\theta_2^{12}=1$, we know that it should have loaded the containers originating in port 1 in week $3-2=1$. The term Cap_s (TEU) refers to the capacity of ship *s*. The right-hand side calculates the capacity of such ship indicated by the tuple (i,k). Note that in constraint set (7), we extend the planning horizon to week $T+m$ to guarantee that the shipping demand near the end of the planning horizon *T* can be satisfied rather than simply ignored because of no ships considered beyond week *T*.

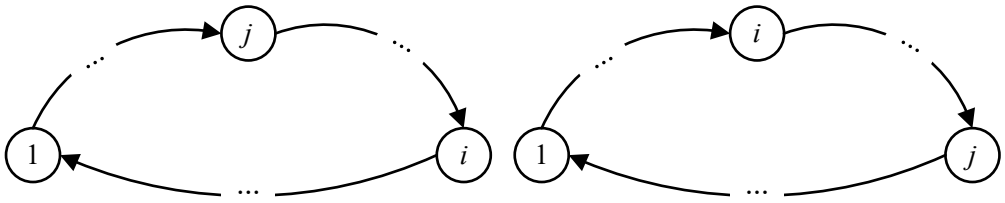

(*a*) (*b*)

Fig. 3. Port rotations of a shipping route, (*a*) $i \geq j$, (*b*) $i < j$

It can be observed that the variable θ_τ^{ji} exists in both sides of the constraint set (7). We now explain how to calculate its value. If $i \geq j$ as shown in Fig. 3(a), the voyage from *j* to *i* does not contain the first port of call 1, that is $j \to j+1 \to ... \to i$. We let I_{ji} represent the set of all ports and legs in the voyage from *j* to *i*. As we consider the time when a ship leaves the first port of call as the start of each voyage, the week differences for a ship to visit port *j* and port *i* can be calculated as

$$\left\lfloor \sum_{h \in I_{1i}} (t_h + t_h^p)/168 \right\rfloor - \left\lfloor \sum_{h \in I_{1j}} (t_h + t_h^p)/168 \right\rfloor \quad (8)$$

where the first and second terms in (8) refer to the number of weeks it takes to visit ports of

call i and j from the first port of call 1 respectively. The operator $\lfloor a \rfloor$ represents the largest integer that is no larger than a. If $i < j$ as shown in Fig. 3(b), the voyage from j to i is $j \to ... \to 1 \to ... \to i$. That is, the ship must visit the port of call 1 before visiting i. Hence the week difference can be calculated as

$$\left\lfloor \sum_{h \in I_{1i}} (t_h + t_h^p) / 168 \right\rfloor - \left\lfloor \sum_{h \in I_{1j}} (t_h + t_h^p) / 168 \right\rfloor + m . \tag{9}$$

We thus have the following two constraint sets for the decision variable θ_τ^{ji}:

$$\sum_{\tau=0}^{m} \tau \theta_\tau^{ji} = \begin{cases} \left\lfloor \sum_{h \in I_{1i}} (t_h + t_h^p) / 168 \right\rfloor - \left\lfloor \sum_{h \in I_{1j}} (t_h + t_h^p) / 168 \right\rfloor, \forall i \geq j \\ \left\lfloor \sum_{h \in I_{1i}} (t_h + t_h^p) / 168 \right\rfloor - \left\lfloor \sum_{h \in I_{1j}} (t_h + t_h^p) / 168 \right\rfloor + m, \forall i < j \end{cases} \quad \forall i, j \in I \tag{10}$$

$$\sum_{\tau=0}^{m} \theta_\tau^{ji} = 1, \quad \forall i, j \in I . \tag{11}$$

3.4 Mixed Integer Nonlinear Programming Model

Denote by c_s^{oper} ($) the ship weekly operating costs except the bunker fuel cost, including the ship weekly maintenance cost, the salary of crews per week, the canal toll fee, the port-stay charge, etc. The total ship operating cost ($) except the bunker fuel cost can be calculated as

$$T \sum_{s \in S} c_s^{oper} x_s . \tag{12}$$

The bunker consumption rate (MT/day) is assumed to be a polynomial function of the sailing speed (knots) of each ship s in the set S, which has been widely adopted in previous studies (e.g., Wang and Meng, 2012b; Brouer et al., 2014; Wang et al., 2015; Meng et al, 2016; Reinhardt et al., 2016; Tierney et al., 2019; Reinhardt et al., 2020)

$$f_i^s(v_i) = \alpha_i^s v_i^{\beta_i^s}, \forall i \in I, s \in S . \tag{13}$$

Substituting $v_i := l_i / t_i$, the function (13) can be rewritten as

$$g_i^s(t_i) = \alpha_i^s l_i^{\beta_i^s} t_i^{1-\beta_i^s} / 24, \forall i \in I . \tag{14}$$

Therefore, the total fuel consumption cost ($) of all ships in T weeks can be expressed as

$$Tc^{bunk} \sum_{s \in S} \sum_{i \in I} \alpha_i^s l_i^{\beta_i^s} t_i^{1-\beta_i^s} x_s / (24m) \tag{15}$$

where c^{bunk} ($/MT) is the bunker fuel price. Let c_{od} ($/TEU) represent the penalty cost for the unsatisfied shipping demand $(o,d) \in D$ and is calculated as the inventory and storage cost, the opportunity cost, the loss of goodwill, and the marginal cost for the container to be transported by other shipping routes of the shipping company itself or other companies. The penalty cost ($) can be thus expressed as

$$\sum_{(o,d) \in D} \sum_{k=1}^{T} c_{od} z_{od}^k . \tag{16}$$

We are now ready to give the mixed integer nonlinear programming model (MINLP) for the DSS problem.

[MINLP] $$\min T \sum_{s \in S} c_s^{oper} x_s + Tc^{bunk} \sum_{s \in S} \sum_{i \in I} \alpha_i^s l_i^{\beta_i^s} t_i^{1-\beta_i^s} x_s / (24m) + \sum_{(o,d) \in D} \sum_{k=1}^{T} c_{od} z_{od}^k \tag{17}$$

Subject to constraint sets (1) ~ (7), (10), (11), and

$$t_i, y_{od}^k, z_{od}^k \geq 0, \forall i \in I, (o,d) \in D, k \in \{1,...,T\} \tag{18}$$

$$x_s, x_s^k, \theta_\tau^{ji} \in \{0,1\}, \forall s \in S, k \in \{1,...,T\}, \tau \in \{0,1,...,m\}, i, j \in I \tag{19}$$

$$m \in Z_+ . \tag{20}$$

The above model is nonlinear because of the nonlinear terms in the objective function (17) and constraint sets (5), (7), and (10). In Section 3.5, we will linearize the nonlinear terms and transform the model to a mixed integer linear programming (MILP) model.

3.5 Model Linearization

It can be easily observed that the decision variable m exists in the index system of constraint sets (5), (7), and (10), which makes the model very hard to deal with. Therefore, we consider enumerating the variable m and solving the **MINLP** model for all possible values of m. Now we have the following model for each value of m.

$$\textbf{[MINLP(}\boldsymbol{m}\textbf{)]}\ \min T\sum_{s\in S}c_s^{oper}x_s + Tc^{bunk}\sum_{s\in S}\sum_{i\in I}\alpha_i^s l_i^{\beta_i^s} t_i^{1-\beta_i^s} x_s / (24m) + \sum_{(o,d)\in D}\sum_{k=1}^{T} c_{od} z_{od}^k \tag{21}$$

Subject to constraint sets (1) ~ (7), (10), (11), (18), and (19).

It should be noted that the following set indicates all possible values of m in the model **MINLP(*m*)**.

$$\left\{\left\lceil \sum_{i\in I}[t_i^p + (l_i / v_i^{\max})] / 168 \right\rceil, ..., \left\lfloor \sum_{i\in I}[t_i^p + (l_i / v_i^{\min})] / 168 \right\rfloor\right\} \tag{22}$$

where the operator $\lceil a \rceil$ calculates the minimum integer that is no less than a.

In the model **MINLP(*m*)**, constraints in the constraint set (5) are linear given each value of m. By introducing two nonnegative continuous auxiliary variables $g_{od}^{ki\tau}$ and $q_s^{ki\tau}$, constraint set (7) can be linearized as follows.

$$\sum_{\substack{(o,d)\in D \\ i\in I_{od}}}\sum_{\tau=0}^{\min\{m,k-1\}} g_{od}^{ki\tau} \le \sum_{s\in S}\sum_{\tau=0}^{\min\{m,k-1\}} q_s^{ki\tau} Cap_s, \forall i\in I, k\in\{1,...,T+m\} \tag{23}$$

$$y_{od}^{k-\tau} + (\theta_\tau^{oi} - 1)\xi_{od}^{k-\tau} \le g_{od}^{ki\tau} \le y_{od}^{k-\tau}, \forall (o,d)\in D, i\in I_{od}, \tau\in\{0,...,\min(m,k-1)\} \tag{24}$$

$$0 \le g_{od}^{ki\tau} \le \theta_\tau^{oi}\xi_{od}^{k-\tau}, \forall (o,d)\in D, i\in I_{od}, \tau\in\{0,...,\min(m,k-1)\} \tag{25}$$

$$0 \le q_s^{ki\tau} \le x_{sk-\tau}^{k-\tau}, \forall i\in I, k\in\{1,...,T+m\}, s\in S, \tau\in\{0,...,\min(m,k-1)\} \tag{26}$$

$$x_s^{k-\tau} + \theta_\tau^{1i} - 1 \le q_s^{ki\tau} \le \theta_\tau^{1i}, \forall i\in I, k\in\{1,...,T+m\}, s\in S, \tau\in\{0,...,\min(m,k-1)\}. \tag{27}$$

By introducing the auxiliary variable $n_i \in \mathrm{Z}_+, i\in I$, constraint set (10) can be linearized as

$$\sum_{\tau=0}^{m}\tau\theta_{\tau}^{ji}=\begin{cases}n_i-n_j,\forall i\geq j\\ n_i-n_j+m,\forall i<j\end{cases}\forall i,j\in I \tag{28}$$

$$n_i\leq\sum_{h\in I_{1i}}(t_h+t_h^p)/168+1/M_1\leq n_i+1,\forall i\in I \tag{29}$$

where M_1 is a very large number. By introducing two nonnegative auxiliary variables B_i^s and C_i^s, the objective function (17) can be linearized as follows.

$$\min T\sum_{s\in S}c_s^{oper}x_s+Tc^{bunk}\sum_{s\in S}\sum_{i\in I}B_i^s/m+\sum_{(o,d)\in D}\sum_{k=1}^{T}c_{od}z_{od}^k \tag{30}$$

$$B_i^s\geq C_i^s+(x_s\text{-}1)M_2,\forall i\in I,s\in S \tag{31}$$

$$C_i^s\geq\alpha_i^s l_i^{\beta_i^s}t_i^{1-\beta_i^s}/24,\forall i\in I,s\in S \tag{32}$$

where the term M_2, a large number, can be set as $\max_{i,s}\{\alpha_i^s l_i(v_i^{\max})^{\beta_i^s-1}/24\}$ here. Constraint set (32) is still nonlinear and can be linearized by the outer linear approximation method widely used in existing studies (e.g. Wang and Meng, 2013; Wang et al., 2019). The linear counterpart of constraint set (32) by this approximation method can be expressed as

$$C_i^s\geq b_{ir}^s+a_{ir}^s t_i,\forall r\in R_i^s,i\in I,s\in S \tag{33}$$

where a_{ir}^s and b_{ir}^s are parameters in the linear approximation constraints; the set R_i^s refers to all linear constraints to approximate the nonlinear constraints (32).

Now the nonlinear model **MINLP(*m*)** can be transformed into the following mixed integer linear programming (MILP) model.

[MILP(*m*)] $$\min T\sum_{s\in S}c_s^{oper}x_s+Tc^{bunk}\sum_{s\in S}\sum_{i\in I}B_i^s/m+\sum_{(o,d)\in D}\sum_{k=1}^{T}c_{od}z_{od}^k \tag{34}$$

subject to constraint sets (1) ~ (6), (11), (18), (19), (23) ~ (29), (31), (33), and

$$g_{od}^{ki\tau},q_s^{ki\tau},B_i^s,C_i^s\geq 0,\forall(o,d)\in D,i\in I,\tau\in\{0,...,m\},k\in\{1,...,T+m\},s\in S \tag{35}$$

$$n_i \in \mathrm{Z}_+, \forall i \in I\,. \tag{36}$$

The above model can be solved by the classical B&C algorithm embedded in state-of-the-art solvers (e.g., CPLEX, Gurobi, and Xpress). However, as will be shown in the numerical experiments in Section 5, due to the large size of the model, it usually takes a very long time to solve the model directly by the B&C for real-sized cases. In this regard, a tailored solution algorithm is developed in the next section to obtain the global optimal solution in a short time.

4. Solution Algorithm

In this section, we develop a tailored solution algorithm to solve the model efficiently. It can be seen that, in the model **MILP(*m*)**, the number of the linearized constraints expressed by (23) ~ (27) for constraint set (7) is very large (i.e., $o(|I||T|m(|D|+|S|))$) which extremely increases the size of the model. Take a case with 10 ports of call and 24 ships as an example, the number of constraints expressed by (23) ~ (27) is 569000 while the number of other constraints in the model is 4983. In other words, the linearization of constraint set (7) greatly increases the solution difficulty of the model. At the same time, we can see that if we fixed θ_τ^{ji} in the model, (7) becomes linear and (23) ~ (27) are no longer needed, which will dramatically reduce the model size and solution difficulty. Based on the above observations, a tailored algorithm is developed to solve the model and can be sketched as follows. We first solve a lower bound (LB) model and obtain the LB value of the problem and a feasible solution of θ_τ^{ji}. Next, we evaluate the feasible solution θ_τ^{ji} by solving the model **MILP(*m*)** by fixing this solution and update the upper bound (UB) value of the problem. Then the feasible solution is removed from the LB model and we resolve the model. This iteration continues until the LB value is larger than the UB value and we get the global optimal solution. This is because all remaining solutions should have objective values larger than the UB and thus do not need to evaluate. In this algorithm, the lower bound model and the **model(*m*)** with the fixed θ_τ^{ji} are iteratively solved. Hence, if both can be solved in a short time, the algorithm will be very efficient to give the optimal solution. In Section 4.1, we will construct a model that is easy to solve and is able to provide a tight lower bound of the model **MILP(*m*)**. In Section 4.2, we will

give the step-by-step description of the tailored solution algorithm, an acceleration method for the algorithm, and the overall algorithm to solve the DSS problem.

4.1 Lower Bound Model

This section constructs an LB model for the model **MILP(*m*)**. We consider two new variables y_{od} and z_{od}, and replace constraint sets (6) and (7) with the following ones:

$$y_{od} + z_{od} \geq \xi_{od}, \forall (o,d) \in D \tag{37}$$

$$\sum_{\substack{(o,d)\in D \\ i \in I_{od}}} y_{od} \leq Cap, \forall i \in I \tag{38}$$

where $\xi_{od} = \min_{k\in\{1,\ldots,T\}} \{\xi_{od}^k\}$ i.e., the lower bound of weekly shipping demand ξ_{od}^k among all weeks, and $Cap = \max_{s\in S}\{Cap_s\}$, i.e., the upper bound of capacities among all ships. Now we obtain the following model.

[LB(*m*)] $$\min T\sum_{s\in S} c_s^{oper} x_s + Tc^{bunk} \sum_{s\in S}\sum_{i\in I} B_i^s / m + T \sum_{(o,d)\in D} c_{od} z_{od} \tag{39}$$

subject to constraint sets (1) ~ (5), (11), (19), (28), (29), (31), (33), (35) ~ (38), and

$$t_i, y_{od}, z_{od} \geq 0, \forall i \in I, (o,d) \in D\,. \tag{40}$$

We can see that as the model **LB(*m*)** does not contain constraint sets (23) ~ (27), it can be efficiently solved by the B&C algorithm. In addition, we have the following proposition for the model **LB(*m*)**.

Proposition 1. *The model **LB(m)** gives a lower bound of the model **MILP(m)**.*

Proof: We first construct a model **LB'(*m*)** by simply replacing the two parameters ξ_{od}^k and Cap_s in the constraint sets (6) and (7) of the model **MILP(*m*)** with $\xi_{od} = \min_{k\in\{1,\ldots,T\}} \{\xi_{od}^k\}$ and $Cap = \max_{s\in S}\{Cap_s\}$ respectively and keep other parameters and constraints unchanged. It is easy to verify that the model **LB'(*m*)** gives a lower bound of the model **MILP(*m*)** because the two constraint set (6) and (7) are relaxed in **LB'(*m*)** and thus **LB'(*m*)** has a larger feasible

region for the decision variables y_{od}^k and z_{od}^k. In addition, it can be observed that in the model **LB'(*m*)**, the shipping demand and ship capacity do not change in all weeks. Therefore, the optimal volume of container shipping demand to satisfy in all weeks should be identical, that is $y_{od}^k = y_{od}^{k-1}$ and $z_{od}^k = z_{od}^{k-1}, \forall k \in \{2,...,T\}$. Therefore, we can equivalently replace the two variables y_{od}^k and z_{od}^k with y_{od} and z_{od}, and obtain the model **LB(*m*)**. This completes the proof.□

4.2 Tailored Solution Algorithm

The step-by-step description of the tailored algorithm to solve the model **MILP(*m*)** is shown in Algorithm 1.

Algorithm 1. *Tailored solution algorithm for the model **MILP(m)***

Input: *m*

Step 1. (*Initialize*) Set the upper bound $UB = \infty$, the lower bound $LB = -\infty$, and the incumbent solution $incum = NULL$.

Step 2. (*Lower bounding*) Solve the model **LB(*m*)**. Set the lower bound as its objective value $LB = Obj_{LB}$ and obtain its optimal solution $\boldsymbol{\theta}^* = \{\theta_\tau^{ji*}, \tau = 0,...,m; i, j \in I\}$.

Step 3. (*Upper bounding*) Solve the model **MILP(*m*)** with the solution $\boldsymbol{\theta}^*$. If the model is infeasible, set $LB = \infty$ and go to Step 5. Otherwise, if $UB > Obj_{MILP}$, set the upper bound $UB = Obj_{MILP}$ and the incumbent solution $incum = \boldsymbol{\theta}^*$.

Step 4. (*Solution removal*) Add the following constraints to the model **LB(*m*)** to exclude the solution $\boldsymbol{\theta}^*$

$$\sum_{(i,j,\tau)\in A(\boldsymbol{\theta}^*)} (1-\theta_\tau^{ji}) + \sum_{(i,j,\tau)\notin A(\boldsymbol{\theta}^*)} \theta_\tau^{ji} \geq 4(|I|-1) \tag{41}$$

where $A(\boldsymbol{\theta}^*) := \{(i,j,\tau) \mid i, j \in I; \tau = 0,...,m; \theta_\tau^{ji*} = 1\}$.

Step 5. (*Convergence check*) If $LB \geq UB$, stop and output the incumbent solution *incum* as the optimal solution and the upper bound *UB* as the optimal objective value; otherwise, go to Step 2.

It is worthwhile to mention that the solution algorithm above can be accelerated. We can see that the lower bound model **LB(*m*)** is iteratively solved in Step 2. When solving the model **LB(*m*)** in each iteration, we usually obtain a series of feasible solutions of $\boldsymbol{\theta}$ on the way to the optimal solution. Therefore, a solution pool can be kept to record these feasible solutions solving the model **LB(*m*)** in Step 2 so that we can evaluate and cut off all of them in Step 3 and Step 4 to expedite the solution process. This makes sense because some feasible solutions in one iteration may be the optimal solutions of the model **LB(*m*)** in subsequent iterations. Therefore, both the UB and LB can be strengthened if these solutions are evaluated and cut off in only one iteration. In addition, another merit of this acceleration method is that only a solution pool is needed to record solutions, which does not increase any computational burden in solving the model **LB(*m*)**. Moreover, evaluating different solutions in the pool in Step 3 can be done in parallel by different processors, which further reduces the solution time. Numerical experiments in Section 5 show that the above acceleration method is able to significantly improve the solution efficiency.

Also, Algorithm 1 shows that this algorithm excludes at least one feasible solution of $\boldsymbol{\theta}$ in each iteration. As the feasible region of $\boldsymbol{\theta}$ defined by constraint sets (10) and (11) is bounded, the number of feasible solutions is finite. Therefore, we have the following proposition for the algorithm.

Proposition 2. *Algorithm 1 gives the global optimal solution in a finite number of iterations.*

Now we are ready to give the solution algorithm to solve the DSS problem with weekly-dependent shipping demand in a shipping route.

Algorithm 2. *Algorithm to solve the DSS problem*

Step 1. (*Initialize*) Set the incumbent solution $incum = NULL$, the incumbent value of the decision variable m $opt\_m = NULL$, and the objective value $Obj = \infty$.

Step 2. (*Enumerating*) For each value of m in the set defined by (22):

Step 2.1. Solve the model **MILP(*m*)** by Algorithm 1. Record the objective value Obj_{MILP} and the optimal solution $\boldsymbol{\theta}^*$.

Step 2.2. If $Obj > Obj_{MILP}$, set $Obj = Obj_{MILP}$, $incum = \boldsymbol{\theta}^*$ and $opt\_m = m$.

Step 3. (*Retrieving solution*) Solve the model **MILP(*m*)** with opt_m and the incumbent solution $incum$. Return the optimal solution t_i^*, $v_i^* := l_i / t_i^*$, x_s^*, x_k^{s*}, y_{od}^{k*}, z_{od}^{k*} together with $incum$, opt_m and the optimal objective value Obj.

5. Numerical Experiments

In this section, numerical experiments based on the real shipping route AEU9 operated by COSCO Shipping are conducted to examine the applicability of the model and the solution efficiency of the tailored solution algorithm developed in this paper. As is shown in Fig. 4, the AEU9 has a total of 10 ports of call, 7 in Asia and 3 in Europe. In these experiments, the capacities of the ships Cap_s are randomly generated in the range $[8000,10000]$ and weekly operating costs c_s^{oper} in the range $[150000,250000]$. The maximum and minimum allowed sailing speeds are $v_i^{\max} = 25$ knots and $v_i^{\min} = 10$ knots respectively. The two parameters α_i^s and β_i^s in the bunker consumption function (13) are generated in the ranges $[0.3,0.7]$ and $[1.7,2.3]$ respectively. In addition, 42 OD pairs of shipping demand are considered. For each OD pair, the number of containers to transport in each week is generated according to actual data and the slot purchase cost is generated as $c_{od} = 100 + [0.2,0.4] \times l_i$ \$/TEU. The bunker price is set to be 300 \$/MT.

In Section 5.1, the efficiency of the algorithm with and without the acceleration method proposed in Section 4.2 is compared to the B&C algorithm in Gurobi. In Section 5.2, the applicability of the model is tested by solving the DSS problem in a real-sized case. Several managerial insights are also obtained to guide shipping operations.

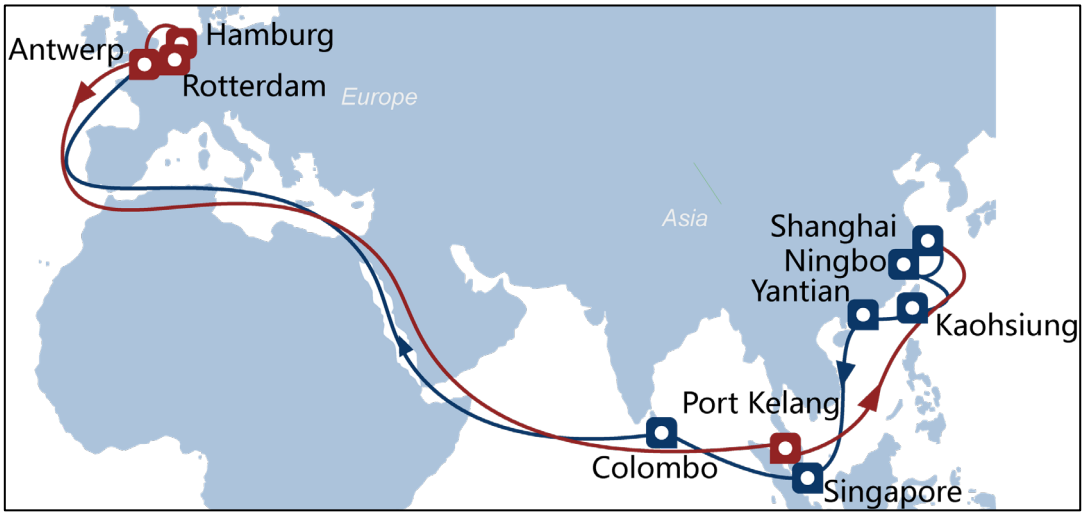

Fig. 4. COSCO AEU9 shipping route

5.1 Efficiency of the tailored solution algorithm

In this section, 35 test instances are generated to examine the efficiency of the tailored solution algorithm. These instances are categorized into 7 groups according to the length of the planning horizons $T \in \{14,18,22,26\}$ and the number of vessels in the candidate set $|S| \in \{12,16,20,24\}$. In addition, the fleet size, *m*, is set to be 12. To compare the solution efficiencies of the tailored algorithm and the B&C algorithm, these test instances are solved by the following three specifications:

(i) directly solved by B&C algorithm in the solver Gurobi;

(ii) solved by the tailored algorithm without the acceleration method in this paper;

(iii) solved by the tailored algorithm with the acceleration method (i.e., evaluate and remove multiple solutions in one iteration).

Table 2. Results of 35 test instances

			MILP model size			B&C/benchmark		Tailored algorithm (w/o acceleration)		Tailored algorithm (with acceleration)	
T	***|S|***	**ID**	**# constrs**	**# cont vars**	**# int vars**	**Gap**	**Time(s)**	**Gap**	**Time(s)**	**Gap**	**Time(s)**
14	12	1	239171	80206	1634	0.00%	1404.57	0.00%	6.35	0.00%	3.37
		2	239171	80206	1634	0.00%	1557.70	0.00%	6.12	0.00%	2.71
		3	239171	80206	1634	0.00%	200.48	0.00%	7.71	0.00%	3.74
		4	239171	80206	1634	0.28%	3600.00	0.00%	7.00	0.00%	2.66
		5	239171	80206	1634	0.00%	227.70	0.00%	3.06	0.00%	1.88
Average in this group						**0.06%**	**1398.09**	**0.00%**	**6.05**	**0.00%**	**2.87**
18	12	1	290907	97702	1682	0.00%	1706.26	0.00%	8.13	0.00%	3.50
		2	290907	97702	1682	0.00%	1914.94	0.00%	6.97	0.00%	2.97
		3	290907	97702	1682	0.00%	187.81	0.00%	0.76	0.00%	0.47
		4	290907	97702	1682	1.17%	3600.00	0.00%	7.69	0.00%	3.28
		5	290907	97702	1682	0.00%	1712.42	0.00%	8.45	0.00%	3.29
Average in this group						**0.23%**	**1824.28**	**0.00%**	**6.40**	**0.00%**	**2.70**
18	16	1	338263	113382	1806	0.00%	488.01	0.00%	16.27	0.00%	7.52
		2	338263	113382	1806	1.17%	3600.00	0.00%	43.38	0.00%	13.58
		3	338263	113382	1806	0.00%	2118.68	0.00%	8.93	0.00%	6.34
		4	338263	113382	1806	0.00%	609.13	0.00%	1.65	0.00%	1.31
		5	338263	113382	1806	1.59%	3600.00	0.00%	43.74	0.00%	17.15
Average in this group						**0.55%**	**2083.16**	**0.00%**	**22.79**	**0.00%**	**9.18**
22	16	1	396255	132958	1870	0.51%	3600.00	0.00%	18.83	0.00%	11.15
		2	396255	132958	1870	0.00%	1864.45	0.00%	37.24	0.00%	14.17
		3	396255	132958	1870	0.00%	421.78	0.00%	45.29	0.00%	12.72
		4	396255	132958	1870	0.71%	3600.00	0.00%	8.61	0.00%	4.68
		5	396255	132958	1870	4.46%	3600.00	0.00%	18.41	0.00%	12.90
Average in this group						**1.14%**	**2617.25**	**0.00%**	**25.68**	**0.00%**	**11.12**
22	20	1	449867	150718	2010	2.66%	3600.00	0.00%	113.88	0.00%	44.28
		2	449867	150718	2010	0.00%	1492.97	0.00%	95.14	0.00%	30.70
		3	449867	150718	2010	0.96%	3600.00	0.00%	21.22	0.00%	14.28
		4	449867	150718	2010	3.35%	3600.00	0.00%	112.30	0.00%	60.61
		5	449867	150718	2010	1.41%	3600.00	0.00%	61.80	0.00%	36.96
Average in this group						**1.68%**	**3178.59**	**0.00%**	**80.87**	**0.00%**	**37.36**
26	20	1	514115	172374	2090	4.13%	3600.00	0.00%	111.99	0.00%	53.48
		2	514115	172374	2090	3.28%	3600.00	0.00%	91.34	0.00%	34.48
		3	514115	172374	2090	0.57%	3600.00	0.00%	113.86	0.00%	45.33
		4	514115	172374	2090	2.53%	3600.00	0.00%	128.97	0.00%	43.39
		5	514115	172374	2090	2.12%	3600.00	0.00%	79.15	0.00%	34.40
Average in this group						**2.52%**	**3600.00**	**0.00%**	**105.06**	**0.00%**	**42.21**
26	24	1	573983	192214	2246	3.61%	3600.00	0.00%	151.41	0.00%	66.55
		2	573983	192214	2246	2.41%	3600.00	0.00%	108.57	0.00%	32.19
		3	573983	192214	2246	4.00%	3600.00	0.00%	105.78	0.00%	42.39
		4	573983	192214	2246	3.01%	3600.00	0.00%	207.50	0.00%	77.39
		5	573983	192214	2246	3.44%	3600.00	0.00%	117.09	0.00%	59.60
Average in this group						**3.29%**	**3600.00**	**0.00%**	**138.07**	**0.00%**	**55.62**
Average of all instances						**1.35%**	**2614.48**	**0.00%**	**54.99**	**0.00%**	**23.01**

The above algorithms are implemented by C++ and call the C++ API of Gurobi to solve the models **MILP(*m*)** and **LB(*m*)**. The computational time limit is 3600 seconds (i.e. 1 hour) for each specification and the target optimality gap is 0. The algorithm stops when either of these two conditions is satisfied.

The detailed results for the above three specifications are shown in Table 2. The columns "#constrs", "#cont vars" and "#int vars" refer to the number of constraints, continuous variables, and integer variables respectively in the model **MILP(*m*)**. The columns "Gap" and "Time" refer to the optimality gap $(UB - LB) / LB$ and the solution time used in each specification respectively. It can be seen that the tailored algorithm is much faster than the B&C algorithm in solving the DSS problem. The B&C algorithm is able to solve only 14 of 35 instances to optimality in 3600 seconds while both the algorithm with and without acceleration are able to solve all 35 instances to optimality. Moreover, the average optimality gap and time used by the B&C of all instances are the largest among the three i.e., 1.35% in 2614.48 seconds while the other two have the average gap 0% in less than 55 seconds. Especially for large instances (e.g., $T = 26$ and $|S| = 20, 24$), the number of constraints in the model is larger than 500000, making the model very difficult to be directly solved by the B&C algorithm (with the gap larger than 2% in 3600s). As a comparison, the tailored algorithm gets optimality in less than 210 seconds. This indicates that the tailored algorithm is able to dramatically reduce the solution difficulty and improve the solution efficiency. In addition, it can be observed that the tailored algorithm with the acceleration method gives a shorter solution time compared with that without acceleration (23.01s vs. 54.99s). This shows that evaluating more than one solution in one iteration is able to improve the upper and lower bounds significantly, thus expediting the convergence and reducing the solution time. At last, we can see that with the increase of the planning horizon, T, and the number of ships $|S|$, the solution times of all three specifications increase. This is because larger T and $|S|$ lead to larger model size and a larger feasible region. Hence, a longer time is needed to calculate the optimal solution. However, we can also observe that the tailored algorithm with acceleration has the smallest increase of the solution time among the three (i.e., from 2.87s to 23.01s vs. from 6.05s to 54.99s and from 1398.09s to

3600s). This indicates that the tailored algorithm with acceleration is the most stable with the variation of the scale of instances.

5.2 Model Application

In this section, to examine the applicability of the model developed in this paper, we consider a real-sized case based on the shipping route AEU9. In this case, 18 candidate ships are available to be deployed and are numbered 1 ~ 18 with the increasing order of ship capacity as shown in Table 3. The planning horizon is 26 weeks (i.e., half a year) because a shipping company usually adjusts its shipping routes no more than half a year. All other parameters in the case are generated similarly to those in Section 5.1.

Table 3. Specifications of 18 ships

Ship No.	Capacity (TEU)	Weekly operating cost ($)	Average bunker consumption rate (the function (13)) with variations of sailing speed (MT/day)			
			10 (knots)	15 (knots)	20 (knots)	25 (knots)
1	8092	174015	40	87	152	236
2	8278	178940	57	130	235	373
3	8302	203968	52	122	223	355
4	8409	222409	55	131	244	395
5	8447	220916	54	125	227	361
6	8577	156151	41	90	160	248
7	8666	155261	43	100	181	288
8	8682	207537	53	124	228	366
9	8804	167414	49	109	195	307
10	8881	219901	65	151	275	439
11	8980	205391	66	155	284	456
12	8984	246784	60	137	247	390
13	9245	160263	40	89	158	247
14	9621	162462	47	103	181	281
15	9696	181265	65	154	283	455
16	9739	206420	55	128	234	374
17	9852	234172	74	179	335	546
18	9861	246511	50	117	214	345

We vary the fleet size, m, according to the set defined by (22) and solve the model **MILP(m)** by Algorithm 1 with acceleration because it has the best performance as shown in Section 5.1. The result is shown in Fig. 5. We can see that with the increase of m, the solution

time first increases and then decreases. This is because when m is very small or very large, the feasible region of the variable defined by constraint sets (2), (10), and (11) is small, leading to a smaller number of iterations in Algorithm 1. On the contrary, the optimal objective value first decreases and then increases. This is because, with the increase of the fleet size, the optimal sailing speed required for the weekly service frequency decreases. At first, the decrease of bunker consumption cost is larger than the increases of total ship operating cost, which leads to the decrease of the total cost. However, as the fleet size continues to increase, the sailing speed cannot reduce largely any more. Therefore, the decrease of bunker consumption cost is lower than the increases of total ship operating cost, which leads to the increase of the total cost. We can see that $m = 9$ leads to the lowest total cost and is the optimal fleet size. We can further determine the optimal ships deployed together with their sequence and sailing speeds by solving the model **MILP(*m*)** with $m = 9$. The optimal sequence of the deployed ships is 16 → 7 → 14 → 13 → 8 → 9 → 1 → 6 → 18. The schedule and sailing speeds of the first ship No.16 are shown in Table 4 and the schedules of other ships can be calculated based on their locations in the sequence. That is, the first ship No.16 starts its journey at Ningbo in time 0h. The second ship No.7 follows 1 week later (i.e., +168h), and then the third ship No. 14 2 weeks later (i.e., +336h) and so forth. The last ship No.18 starts the journey 8 weeks later (i.e., +1344 h). After that, the first ship No. 16 returns to Ningbo and starts a new journey 9 weeks later (i.e., +1512 h). This continues until the end of the planning horizon. The schedules of other deployed ships at other ports can be calculated accordingly.

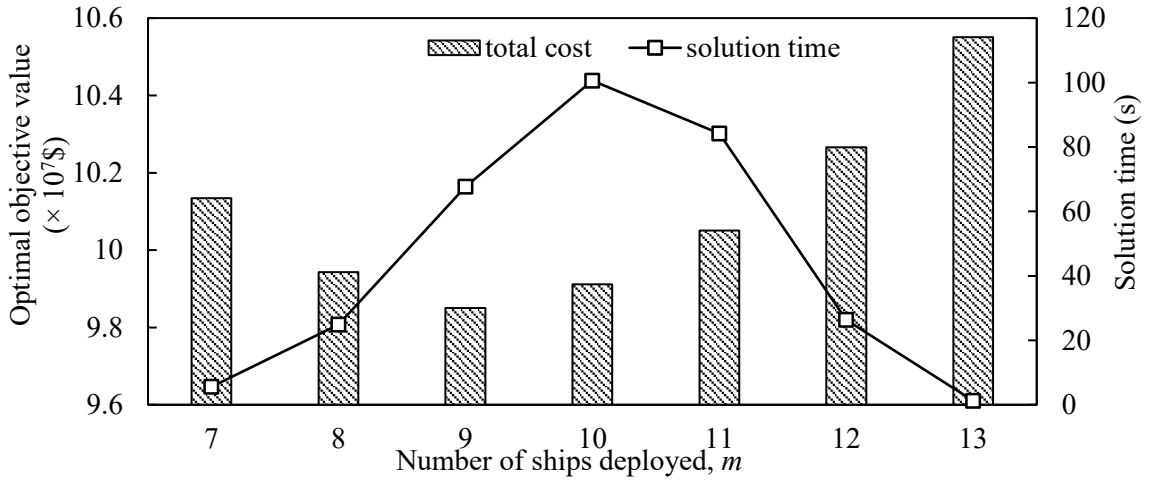

Fig. 5. The optimal objective value and solution time of the model MILP(m) by Algorithm 1

Table 4. Schedule of the first ship (No.11)

Port/Leg	Arrival time (h)	Departure time (h)	Cumulative distance (nautical mile)	Sailing speed (knots)	Sailing time (h)
Ningbo→	-	0	0	12	8
Shanghai→	8	28	93	13	43
Kaohsiung→	71	84	639	13	25
Yantian→	109	124	974	18	78
Singapore→	202	220	2405	15	104
Colombo→	325	339	3965	16	412
Antwerp→	750	767	10729	15	25
Hamburg→	792	804	11099	14	22
Rotterdam→	826	838	11399	17	492
Port Kelang→	1330	1344	19530	14	154
Ningbo→	1498	1512	21732	-	-

We also compare the performance of the model developed in this paper with the model that considers homogenous vessels. In the model with homogeneous vessels, the capacity Cap_s, the operating cost c_s^{oper}, and the bunker consumption parameters α_i^s, β_i^s of all vessels are identical and equal to the average of the corresponding parameters in our model with heterogeneous vessels. Besides, the shipping demand for each OD pair in each week equals the average shipping demand ξ_{od}^k across the planning horizon in our model. That is, that model considers the weekly independent shipping demand. The optimal solution is shown in Table 5. It can be seen that compared with the model with homogeneous vessels, considering heterogeneous vessels in our model gives a smaller fleet size (with the variation of 10%) and a much lower ship operating cost (with the variation of 17.04%). This indicates that our model is able to fully incorporate the uniqueness of different vessels to give a smart fleet deployment to reduce the ship operating cost. Moreover, due to the smaller fleet size, the sailing speed of ships in our model is higher, which leads to a higher bunker fuel consumption cost (5.2195×10^7\$ vs. 5.0349×10^7\$). In addition, our model transports slightly fewer containers than the model with homogenous vessels, and 2199-TEU containers should be transported by other sources. This can be explained that in our model, deploying smaller ships with a lower operating cost leads to a lower total cost. Finally, the total cost in our model is lower than that with homogenous vessels (with a variation of 3.08%). This shows the power of the model with

heterogeneous vessels. Considering the low profit margin of the shipping companies (usually less 5%), a 3% reduction of total cost indicates a significant improvement in their profitability.

Table 5. Comparison between models with homogenous and heterogeneous vessels

Model	Fleet size	Ship operating cost ($\times 10^7$\$)	Bunker fuel cost ($\times 10^7$\$)	Transported containers ($\times 10^5$TEU)	Unsatisfied containers (TEU)	Total cost ($\times 10^7$\$)
Homogenous vessels	10	5.1275	5.0349	4.3687	0	10.1624
Heterogeneous vessels	9	4.2537	5.2195	4.3467	2199	9.8499
Variation	-10.00%	-17.04%	3.67%	-0.50%	-	-3.08%

We turn to investigate the effects of the variations of some important parameters on the model solutions. We first vary the bunker price c^{bunk} from 100 \$/MT to 600 \$/MT and keep other parameters unchanged. The results are given in Table 6. It can be seen that with the increase of the bunker price, the optimal fleet size and the total ship operating cost increase from 7 to 13 and from 3.0920×10^7\$ to 6.2949×10^7\$ respectively. This is because the increase of the bunker price reduces the optimal sailing speed (from 21.16 knots to 11.68 knots) and thus increases the total round-trip time. To maintain fixed service frequency, more ships should be deployed in this route. In addition, the ships deployed and their sequences are also changed. For example, when bunker price increases from 100 \$/MT to 200 \$/MT, the ships No. 15 and No. 16 are replaced with ships No. 1 and No.18. This is because, with the increase of the bunker price, the operators need to deploy ships with higher fuel efficiency in the shipping route. Moreover, with the reduction of the sailing speed, the amount of bunker fuel consumed decreases (from 2.4463×10^5MT to 1.2465×10^5MT) but the total bunker fuel cost increases (from 2.4463×10^7\$ to 7.4792×10^7\$) due to the increase of the bunker price. It can be also observed that the variation of the bunker price seldom affects the number of containers transported. Finally, the increase of bunker price leads to an increase of the total cost from 5.7217×10^7\$ to 14.3349×10^7\$.

We now vary the shipping demand volume of each OD pair ξ_{od}^k as 0.5, 0.8, 1.0, 1.5, and 2.0 times of the benchmark value. The effect of the shipping demand variations on the optimal solution is shown in Table 7. It can be observed that when the volume of shipping

demand increases, the fleet size decreases a little (from 9 to 8), but the ship operating cost increases (from 4.0716×10^7\$ to 4.1738×10^7\$). This is because, in order to satisfy the increasing container shipping demand, larger ships are deployed to transport more containers but with a larger operating cost and more bunker fuel consumption. For example, when the shipping demand increases from "×1.5" to "×2.0", ship No. 6 with the capacity of 8577 TEUs and weekly operating cost of 156151\$ is replaced with ship No. 12 with the capacity of 8984 TEUs and weekly operating cost of 246784\$. In addition, with the reduction of fleet size, these remaining large ships complete more voyages in the planning horizon to transport more containers and a higher sailing speed (15.94 knots vs. 18.19knots) is needed to maintain fixed service frequency. Finally, with the increase of the shipping demand volume, the unsatisfied shipping demand also increases (from 0 to 362331 TEU), which leads to a higher total cost (from 9.3275×10^7\$ to 92.5415×10^7\$ 一般都是写成\$$92.5415\times10^7$，见 https://www.really-learn-english.com/dollar-sign.html).

At last, we explore the effect of the variations of the ship weekly operating cost c_s^{oper} on the optimal solution. Similarly, we vary the weekly operating cost as 0.5, 0.8, 1.0, 1.5, and 2.0 times of the benchmark value. It can be seen from Table 8 that the increase of the weekly operating cost leads to a smaller fleet size (from 12 to 7) but a higher total ship operating cost (from 2.9503×10^7\$ to 6.3548×10^7\$). For example, when the ship weekly operating cost increases from "×0.8" to "×1.0", ship No. 15 is removed from the shipping route to hedge the increase of the total ship operating cost. Therefore, the sailing speed increases (from 11.64 knots to 21.16 knots) to maintain weekly service frequency and also the bunker fuel cost (4.1671×10^7\$ to 6.3848×10^7\$). In addition, the unsatisfied shipping demand increases (from 1508 TEU to 3317 TEU) due to the removal of large ships with high operating costs from the shipping route. Finally, we have a higher total cost (7.3763×10^7\$ vs. 13.3116×10^7\$) because of the increase of ship operating cost, bunker fuel cost, and the penalty cost for the unsatisfied demand.

Table 6. Effect of bunker price on the optimal solution

Bunker price c^{bunk} ($/MT)	Fleet size	Ship operating cost (×10^7$)	Average sailing speed (knots)	Bunker fuel amount (×10^{5}MT)	Bunker fuel cost (×10^7$)	Transported containers (×10^{5}TEU)	Total cost (×10^7$)	Sequence of deployed ships →												
100	7	3.0920	21.16	2.4463	2.4463	4.3585	5.7217	15	14	6	13	9	16	7						
200	7	3.1774	21.16	2.1525	4.3051	4.3388	7.9940	7	18	1	13	9	6	14						
300	9	4.2537	15.94	1.7398	5.2195	4.3467	9.8499	16	7	14	13	8	9	1	6	18				
400	10	4.7840	14.19	1.5677	6.2710	4.3412	11.5268	16	6	9	7	13	1	3	18	14	8			
500	12	5.7205	12.64	1.3493	6.7464	4.3380	12.9883	18	2	6	13	3	7	14	15	1	8	9	16	
600	13	6.2949	11.68	1.2465	7.4792	4.3355	14.3349	2	15	3	5	14	16	9	8	6	18	13	1	7

Table 7. Effect of shipping demand variations on the optimal solution

Shipping demand ξ_{od}^k	Fleet size	Ship operating cost (×10^7$)	Average sailing speed (knots)	Bunker fuel cost (×10^7$)	Transported containers (×10^{5}TEU)	Unsatisfied containers (TEU)	Total cost (×10^7$)	Sequence of deployed ships →								
× 0.5	9	4.0716	15.94	5.2559	2.1843	0	9.3275	9	8	7	3	1	14	2	6	13
× 0.8	9	4.0716	15.94	5.2559	3.4949	0	9.3275	9	8	7	3	1	14	2	6	13
× 1.0	9	4.2537	15.94	5.2195	4.3467	2199	9.8499	16	7	14	13	8	9	1	6	18
× 1.5	8	3.9381	18.19	6.9916	5.0184	153461	41.7437	17	13	14	9	16	18	15	6	
× 2.0	8	4.1738	18.19	7.3744	5.1140	362331	92.5415	17	15	13	12	16	18	14	9	

Table 8. Effect of ship weekly operating cost variations on the optimal solution

Weekly operating cost c_s^{oper}	Fleet size	Ship operating cost (×10^7$)	Average sailing speed (knots)	Bunker fuel cost (×10^7$)	Transported containers (×10^{5}TEU)	Unsatisfied containers (TEU)	Total cost (×10^7$)	Sequence of deployed ships →											
× 0.5	12	2.9503	11.64	4.1671	4.3536	1508	7.3763	14	1	6	18	16	11	13	15	7	8	9	12
× 0.8	10	3.7800	14.20	4.8537	4.3493	1931	8.9662	13	6	9	7	14	1	15	18	16	8		
× 1.0	9	4.2537	15.94	5.2195	4.3467	2199	9.8499	16	7	14	13	8	9	1	6	18			
× 1.5	7	4.7661	21.16	6.3848	4.3355	3317	11.7229	14	13	1	18	9	6	7					
× 2.0	7	6.3548	21.16	6.3848	4.3355	3317	13.3116	14	13	1	18	9	6	7					

6. Conclusions

Most existing studies on the operation management of liner container shipping assume identical container ships in a shipping route. However, in real operations, these container ships deployed in a shipping route usually differ in the ship capacity, operating cost, bunker fuel efficiency, etc. The distinction among these ships can be so significant that a wise ship deployment and scheduling could lead to substantial cost savings. This paper thus considers the deployment, sequencing, and scheduling problem for the heterogeneous vessels in a liner container shipping route. To select the optimal ships from a set of candidate ships available to deploy in the route and determine their visit sequence, sailing speed, and schedule, a mixed integer programming model is constructed to minimize the total cost which includes the ship operating cost, the bunker fuel cost, and the penalty cost of unsatisfied shipping demand due to ship capacities. Because of the large size of the model, the classical B&C algorithm in existing solvers cannot calculate the optimal solution in a short time. Therefore, a tailored solution algorithm is developed in this paper that is able to obtain the global optimal solution efficiently in a finite number of iterations. This algorithm first constructs and solves a lower bound problem to obtain a feasible solution and the LB of the optimal solution of the original model. Then this feasible solution is evaluated in the original model to update the UB. This lower bound problem is resolved after the feasible solution is removed to obtain a new feasible solution. This continues until the LB exceeds the UB. A series of numerical experiments are conducted to examine the efficiency of the algorithm and the applicability of the optimization model. The experiment results can be summarized as follows:

(i) The tailored solution algorithm outperforms the classical B&C algorithm in all test instances. The solution time of the tailored solution algorithm can be up to 2~3 orders of magnitude lower than that of the B&C algorithm. In addition, the acceleration technique considered in this paper is able to further improve the solution efficiency of the algorithm.

(ii) The model considering heterogeneous vessels developed in this paper is compared with that considering homogenous vessels. Results show that this model leads to a cost saving of 3%, a significant reduction considering that the liner shipping industry is capital intensive.

(iii) The bunker fuel price, shipping demand volume, and ship weekly operating cost have significant effects on the optimal deployment strategy, sequence, and schedule of the heterogeneous vessels. In detail, we have the following results:

a) The increase of the bunker price increases the fleet size and reduces the sailing speed. The fuel-efficient ships are adopted to hedge the rising of bunker fuel cost.

b) The increase of the demand shipping volume leads the shipping company to adopt larger ships, resulting in the rise of the total ship operating cost. The ship sequence also changes significantly with the variation of the shipping demand volume.

c) The increase of the ship weekly operating cost not only raises the total operating cost but also reduces the volume of satisfied shipping demand due to the removal of large ships with a high operating cost from the fleet.

Future research can be conducted in the following two aspects. First, this paper considers the deterministic shipping demand. However, in actual shipping operations, the shipping demand may fluctuate and can be viewed as a stochastic variable. Hence, future research can consider the random shipping demand in each week and construct a multi-stage stochastic programming model to solve the DSS problem. Second, only a single route is considered in this paper. As a shipping company usually transport containers in a shipping network that consists of several routes, future research can consider the DSS problem in the shipping network level.

Acknowledgment

We are very grateful to the editor and three anonymous reviewers for their helpful comments and suggestions on earlier versions of the paper.

References

Abioye, O. F., Dulebenets, M. A., Kavoosi, M., Pasha, J., & Theophilus, O. (2020). Vessel Schedule Recovery in Liner Shipping: Modeling Alternative Recovery Options. *IEEE Transactions on Intelligent Transportation Systems*, 1-15.

Agarwal, R., & Ergun, Ö. (2008). Ship scheduling and network design for cargo routing in liner shipping. *Transportation Science*, *42*(2), 175-196.

Alvarez, J. F. (2009). Joint routing and deployment of a fleet of container vessels. *Maritime Economics & Logistics*, *11*(2), 186-208.

Aydin, N., Lee, H., & Mansouri, S. A. (2017). Speed optimization and bunkering in liner shipping in the presence of uncertain service times and time windows at ports. *European Journal of Operational Research*, *259*(1), 143-154.

Benford, H. (1981). A simple approach to fleet deployment. *Maritime Policy and Management*, *8*(4), 223-228.

Brouer, B. D., Alvarez, J. F., Plum, C. E., Pisinger, D., & Sigurd, M. M. (2014). A base integer programming model and benchmark suite for liner-shipping network design. *Transportation Science*, *48*(2), 281-312.

Cheaitou, A., & Cariou, P. (2019). Greening of maritime transportation: a multi-objective optimization approach. *Annals of Operations Research*, 273(1-2), 501-525.

COSCO (2020). Europe-AEU1. < http://lines.coscoshipping.com/home/Services/route /12> . (Accessed 5 August 2020)

Dulebenets, M. A. (2018). The vessel scheduling problem in a liner shipping route with heterogeneous fleet. *International Journal of Civil Engineering*, *16*(1), 19-32.

Dulebenets, M. A., & Ozguven, E. E. (2017). Vessel scheduling in liner shipping: Modeling transport of perishable assets. *International Journal of Production Economics*, *184*, 141-156.

Dulebenets, M. A., Pasha, J., Abioye, O. F., & Kavoosi, M. (2019). Vessel scheduling in liner shipping: a critical literature review and future research needs. *Flexible Services and Manufacturing Journal*, in press.

Fagerholt, K. (2001). Ship scheduling with soft time windows: An optimisation based approach. *European Journal of Operational Research*, *131*(3), 559-571.

Fagerholt, K., Johnsen, T. A., & Lindstad, H. (2009). Fleet deployment in liner shipping: a case study. *Maritime Policy & Management*, *36*(5), 397-409.

Fagerholt, K., & Psaraftis, H. N. (2015). On two speed optimization problems for ships that sail in and out of emission control areas. *Transportation Research Part D: Transport and Environment*, *39*, 56-64.

Gelareh, S., & Meng, Q. (2010). A novel modeling approach for the fleet deployment problem within a short-term planning horizon. *Transportation Research Part E: Logistics and Transportation Review*, *46*(1), 76-89.

Giovannini, M., & Psaraftis, H. N. (2019). The profit maximizing liner shipping problem with flexible frequencies: logistical and environmental considerations. *Flexible Services and Manufacturing Journal*, 31(3), 567-597.

Gürel, S., & Shadmand, A. (2019). A heterogeneous fleet liner ship scheduling problem with port time uncertainty. *Central European Journal of Operations Research*, 27(4), 1153-1175.

Meng, Q., Du, Y., & Wang, Y. (2016). Shipping log data based container ship fuel efficiency modeling. Transportation Research Part B: Methodological, 83, 207-229.

Meng, Q., & Wang, S. (2012). Liner ship fleet deployment with week-dependent container shipment demand. *European Journal of Operational Research*, *222*(2), 241-252.

Meng, Q., & Wang, T. (2010). A chance constrained programming model for short-term liner ship fleet planning problems. *Maritime Policy and Management*, *37*(4), 329-346.

Meng, Q., Wang, T., & Wang, S. (2012). Short-term liner ship fleet planning with container transshipment and uncertain container shipment demand. *European Journal of Operational Research*, *223*(1), 96-105.

Monemi, R. N., & Gelareh, S. (2017). Network design, fleet deployment and empty repositioning in liner shipping. *Transportation Research Part E: Logistics and Transportation Review*, *108*, 60-79.

Ng, M.W. (2014). Distribution-free vessel deployment for liner shipping. *European Journal of Operational Research*, *238*(3), 858-862.

Ng, M.W. (2015). Container vessel fleet deployment for liner shipping with stochastic dependencies in shipping demand. *Transportation Research Part B: Methodological*, *74*, 79-87.

Pasha, J., Dulebenets, M. A., Kavoosi, M., Abioye, O. F., Theophilus, O., Wang, H., ... & Guo, W. (2020). Holistic tactical-level planning in liner shipping: an exact optimization approach. *Journal of Shipping and Trade*, 5, 1-35.

Perakis, A. N. (1985). A second look at fleet deployment. *Maritime Policy and Management*, *12*(3), 209-214.

Powell, B. J., & Perkins, A. N. (1997). Fleet deployment optimization for liner shipping: An integer programming model. *Maritime Policy and Management*, *24*(2), 183-192.

Reinhardt, L. B., Pisinger, D., Sigurd, M. M., & Ahmt, J. (2020). Speed optimizations for liner networks with business constraints. *European Journal of Operational Research*, 285(3), 1127-1140.

Reinhardt, L. B., Plum, C. E., Pisinger, D., Sigurd, M. M., & Vial, G. T. (2016). The liner shipping berth scheduling problem with transit times. *Transportation Research Part E: Logistics and Transportation Review*, 86, 116-128.

Ronen, D. (2011). The effect of oil price on containership speed and fleet size. *Journal of the Operational Research Society*, *62*(1), 211-216.

Song, D. P., & Dong, J. X. (2013). Long-haul liner service route design with ship deployment and empty container repositioning. *Transportation Research Part B: Methodological*, *55*, 188-211.

Song, D. P., Li, D., & Drake, P. (2015). Multi-objective optimization for planning liner shipping service with uncertain port times. *Transportation Research Part E: Logistics and Transportation Review*, *84*, 1-22.

Tan, Z., Wang, Y., Meng, Q., & Liu, Z. (2018). Joint ship schedule design and sailing speed optimization for a single inland shipping service with uncertain dam transit time. *Transportation Science*, *52*(6), 1570-1588.

Tierney, K., Ehmke, J. F., Campbell, A. M., & Müller, D. (2019). Liner shipping single service design problem with arrival time service levels. *Flexible Services and Manufacturing Journal*, 31(3), 620-652.

UNCTAD (2019). Review of Maritime Transportation 2019. Paper presented at the United Nations Conference on Trade and Development. New York and Geneva. <https://unctad.org/en/PublicationsLibrary/rmt2019_en.pdf>. (Accessed 5 August 2020).

Wang, S. (2015). Optimal sequence of container ships in a string. *European Journal of Operational Research*, *246*(3), 850-857.

Wang, S., & Meng, Q. (2012a). Liner ship fleet deployment with container transshipment operations. *Transportation Research Part E: Logistics and Transportation Review*, *48*(2), 470-484.

Wang, S., & Meng, Q. (2012b). Sailing speed optimization for container ships in a liner shipping network. *Transportation Research Part E: Logistics and Transportation Review*, 48(3), 701-714.

Wang, S., & Meng, Q. (2017). Container liner fleet deployment: a systematic overview. *Transportation Research Part C: Emerging Technologies*, *77*, 389-404.

Wang, Y., Meng, Q., & Du, Y. (2015). Liner container seasonal shipping revenue management. *Transportation Research Part B: Methodological*, *82*, 141-161.

Wang, Y., Meng, Q., & Kuang, H. (2018). Jointly optimizing ship sailing speed and bunker purchase in liner shipping with distribution-free stochastic bunker prices. *Transportation Research Part C: Emerging Technologies*, 89, 35-52.

Wang, Y., Meng, Q., & Kuang, H. (2019). Intercontinental liner shipping service design. *Transportation Science,* 53(2), 344-364.

Wang, Y., & Meng, Q. (2020). Semi-liner Shipping Service Design. *Transportation Science*, 54(5), 1288-1306.

Xia, J., Li, K. X., Ma, H., & Xu, Z. (2015). Joint planning of fleet deployment, speed optimization, and cargo allocation for liner shipping. *Transportation Science*, *49*(4), 922-938.

Zhen, L., Wang, S., Laporte, G., & Hu, Y. (2019). Integrated planning of ship deployment, service schedule and container routing. *Computers & Operations Research*, 104, 304-318.

Zhen, L., Hu, Y., Wang, S., Laporte, G., & Wu, Y. (2019). Fleet deployment and demand fulfillment for container shipping liners. *Transportation Research Part B: Methodological*, *120*, 15-32.

Zhu, M., Yuen, K. F., Ge, J. W., & Li, K. X. (2018). Impact of maritime emissions trading system on fleet deployment and mitigation of CO_2 emission. *Transportation Research Part D: Transport and Environment*, *62*, 474-488.